Synthetic Metals, 23 (1988) 113–119

INCOMMENSURATE STRUCTURES OF OsF_6 AND MoF_6 GRAPHITE INTERCALATES STUDIED BY NEUTRON SCATTERING

J.K. KJEMS*
Riso National Laboratory, DK-4000 Roskilde (Denmark)
D. VAKNIN**, D. DAVIDOV and H. SELIG
Hebrew University, Jerusalem (Israel)
Y. YESHURUN
Bar-Ilan University, Ramat-Gan (Israel)

ABSTRACT

Neutron scattering has been used to study the in-plane structure of stage-1 graphite intercalated $C_{8.4}MoF_6$ and C_9OsF_6. Both compounds exhibit a first order phase transition at 280K from a liquid to a modulated 2D incommensurate structure at low temperatures. The structure can be described as a domain-wall modulated $(2x2)R\alpha^{O}$ where α is a small rotation angle. In $C_{8.4}MoF_6$ the domain-wall lattice is correlated over 250Å which is close to the instrumental resolution, whereas for the C_9OsF_6 the correlation range is only 60Å. The relation between the residual resistivity and the intercalant structure is discussed.

INTRODUCTION

Graphite intercalation compounds with metal hexafluorides, HOPG/MoF_6 and HOPG/OsF_6, have been extensively studied in the past several years using ESR [1], susceptibility [2], reflectivity [3] and in-plane and c-axis resistivities [4]. It was found that the charge transfer per intercalant species is one electron for stage I C_9OsF_6 but only 0.2 electrons for stage I $C_{8.4}MoF_6$ [1,2]. The charge transfer per carbon atom, however, is only slightly larger for the former GIC, suggesting possible charge localization [3]. The in-plane residual resistivity for C_9OsF_6 (stage I) was found to be larger than that of $C_{8.4}MoF_6$ by several orders of magnitude.

---

* Invited paper.

** Present address: Physics Department, Brookhaven National Laboratory, Upton, Long Island, N.Y.

0379-6779/88/$3.50

Here we present neutron diffraction and in-plane resistivity data, for stage I C_9OsF_6 and $C_{8.4}MoF_6$. The in-plane structure is modulated by domains and domain walls due to strong coupling with the graphite lattice. We demonstrate a correlation between the intercalant domain size and the residual resistivities.

EXPERIMENTAL DETAILS AND RESULTS

Sample Preparation

Samples were prepared from HOPG and characterized by methods described previously [1,2].

Neutron diffraction

The neutron diffraction experiments were carried out using a triple axis spectrometer situated at a cold source beam at the Riso Dr-3 reactor. For the

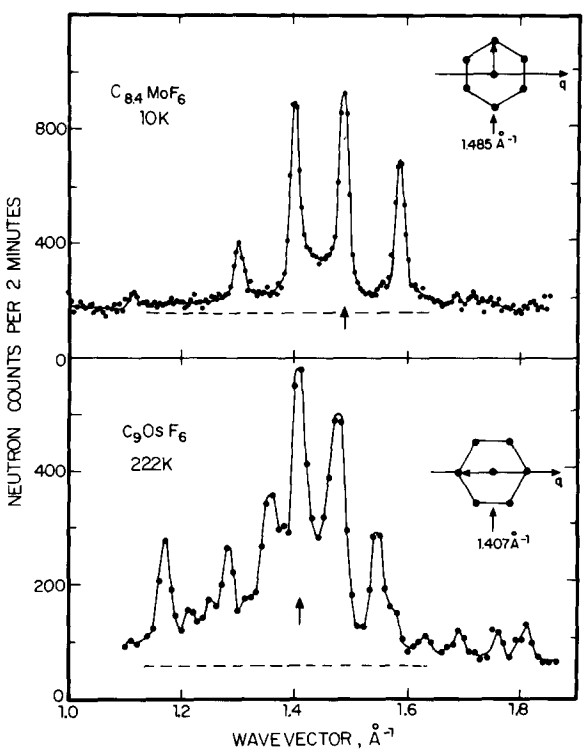

FIG. 1. High resolution neutron diffraction scans with momentum transfer in the plane for $C_{8.4}MoF_6$ and C_9OsF_6. The full line is a guide to the eye and the broken line indicates the level of background scattering. Note that for C_9OsF_6 the spectrum is temperature independent from 250K down to 4K. The inserts illustrate the satellite patterns near the $\tau_I(10)$ reflections which give a satisfactory assignment of the observed peaks. The arrows indicate the positions for the fundamental peaks of the intercalant structure.

initial scans a wavelength of 2.38Å was used, at which pyrolytic graphite filters are very efficient in removing any higher order contamination. High resolution scans were performed using wavelength of 4Å and 4.3Å. A 10-cm cooled Be-filter placed before the graphite (002) monochromator and, in the latter case, combined with a 5 cm graphite filter, was used to remove the higher orders. The typical collimation was 60', but occasionally 30' was used before the monochromator and after the sample. The best resolution achieved was $0.0095Å^{-1}$, full width at half maximum (FWHM). The samples were mounted in standard sealed aluminum containers, filled with He in a dry box. The c-axis was in the scattering plane and the cooling was achieved by means of a closed cycle refrigerator.

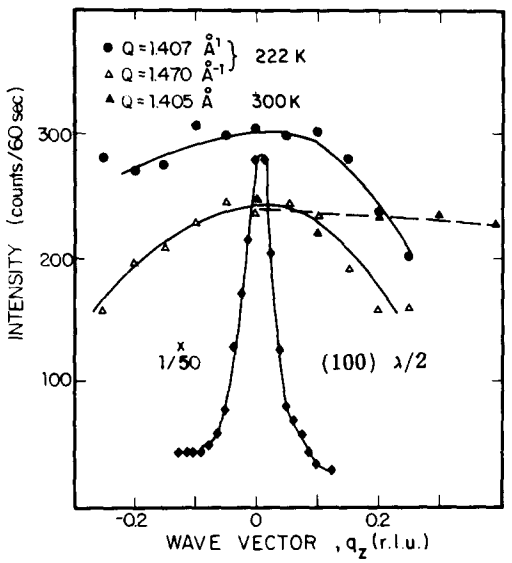

FIG. 2. Scans along q_z for the most prominent in-plane peaks for C_9OsF_6 together with a similar scan for the $\tau(100)\lambda/2$ reflection. The weak q_z dependence corresponds to 2D nature of the intercalant structure.

The staging index and the A-A stacking of the carbon layers were confirmed by measurements of several of the fundamental graphite reflections. The intercalant structure is seen most clearly in the in-plane scans and Fig. 1 shows examples of such scans in the low temperature phases of the two compounds. The most intense scattering is found in the wavevector region $1Å^{-1} < q < 2Å^{-1}$. The region $2Å^{-1} < q < 3Å^{-1}$ contained very little intercalant scattering in accordance with calculations of the average form factor of the MF_6^- molecules. Weak intercalant peaks were observed in the range $3Å^{-1} < q < 4Å^{-1}$, but we were unable to assign those. Scans along q_z for the most prominent in-plane intercalant peaks for C_9OsF_6 are shown in Fig. 2 together with similar scans of the $\tau_G(100)$, $\lambda/2$ whose width in q_z is determined by the mosaic of the sample. Clearly the

intercalant peaks are much broader, which is a signature of the 2-D nature of the low temperature structure of the compounds. Similar results were obtained for HOPG/MoF_6. The intercalant structures become disordered above 280K and the temperature evolution of the diffraction patterns and of the c-axis resistivity was followed in detail through the transition region from 30K upwards. Both types of measurements show hysteresis and, furthermore, the low temperature diffraction patterns were found to be dependent on the thermal history. However, slow cooling (<0.5K/min.) from the fully disordered state gave reproducible results.

Resistivity Measurements

The in-plane resistivity was measured by a contactless method using a ferrite core adapted to a helium flux system [4]. Figs. 3 present the in-plane resistivity as a function of temperature for some of the compounds. The resistivity data were fitted to the relation $\rho_a = A+BT+CT^2$ and the various parameters are given in Table 1 for some of the samples.

TABLE I

	A ($\mu\Omega$ cm)	B $\mu\Omega$ cm/K	C $\mu\Omega$ cm/K^2
C_9OsF_6 (I)	100	---	---
$C_{12}OsF_6$ (I)	28.0	2.8×10^{-2}	2.5×10^{-4}
C_9MoF_6 (I)	0.6	5×10^{-4}	5×10^{-5}
$C_{10}MoF_6$ (I)	1.95	2×10^{-3}	5×10^{-5}

The most striking feature is the significantly larger residual resistivity for C_9OsF_6 as compared to C_9MoF_6. Using a Drude type model we have estimated a mean free path length, L, of L = 20Å for C_9OsF_6 and L = 3000Å for C_9MoF_6. The tunneling model of Ulloa and Kirczenow [5] gives a domain size of L(DH) = 20Å for C_9OsF_6 and L(DH) = 3020Å assuming a wall thickness of 8Å.

Structural Model

The observed diffraction patterns at low temperatures can be interpreted in terms of a model based on a close-packed 2-D intercalant lattice (neglecting molecular orientation effects) with a lattice parameter, a_I, near that of the (2x2)-registered structure. For C_9OsF_6 the lattice mismatch, ($a_G/2a_I$) is 0.950, whereas it is very close to 1.0 for $C_{8.4}MoF_6$. The harmonic interaction between the graphite and the intercalant lattices induce a modulation pattern with characteristic Fourier-components given by $\tau_s = \tau_G - \tau_I$, where τ_G denotes a reciprocal lattice vector associated with the graphite layers, and τ_I denotes the corresponding vectors of the intercalant lattice [6]. The modulation pattern gives rise to a decoration of the fundamental reflection of both lattices with a

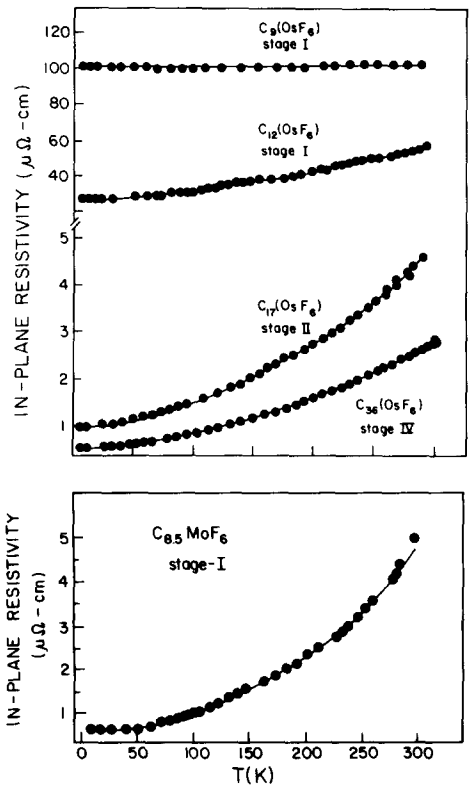

FIG. 3. The temperature dependence of the in-plane conductivities for different stages C/OsF_6 and for stage I $C_{8.5}MoF_6$

hexagonal pattern of satellite reflections. The satellite intensities reflect the actual distortions. In the q-range shown in Fig. 1 we observe mainly the satellites near the $\tau_I(10)$-reflection in a projection onto the q-axis, due to the powder average in the plane. The simplest assignment of these peaks can be made on the basis of the satellite patterns shown schematically as inserts in Fig. 1. With this assignment we deduce that the MoF_6-intercalant lattice is very near to (2x2)-registry and that the small mismatch in the lattice parameters gives rise to a rotational epitaxy dominated by transverse modulations. The modulation vector is $|\tau_s| = 0.106\text{Å}^{-1}$ which corresponds to a relative rotation of the graphite and the intercalant lattices of $\alpha = 2.8°$. The larger lattice parameter mismatch for the OsF_6-compound results in the modulation pattern of predominantly longitudinal character where the length of the modulation vector $|\tau_s| = 0.125\text{Å}^{-1}$ is close to the lattice mismatch. In both cases the modulation pattern can be thought of as a domain-wall lattice with domains of linear dimensions $1/|\tau_s|$ corresponding to 20-25 a_G-units. The domains are separated by fairly sharp domain walls as can be deduced from the facts that (1) the satellites are as intense as the fundamental reflections, and (2) satellites up to

high orders are observed. However, a more quantitative analysis will require accurate single crystal structure factor data. A closer examination of the peak positions shows that they deviate systematically from the simple assignment based on the harmonic model, especially for the OsF_6-compound. We interepret this as evidence for distortions of the domain-wall lattices, probably due to higher-order registry effects. In Table 2 we list the calculated peak positions

TABLE 2
Comparison of the observed and calculated peak positions for the domain-wall lattices in C_9OsF_6 and $C_{8.4}MoF_6$. Model (1) is hexagonal and models (2) and (3) have orthorhombic distortions. For further detals see Ref. [6]. All the values are in $Å^{-1}$ units.

	Observed positions	model 1	model 2	model 3
C_9OsF_6	1.169	1.169	1.1701	1.170
τ_s = 0.125	1.277	1.289	1.284	1.281
	1.360	1.352	1.369 + 1.337	1.340 + 1.353
τ_I = 1.407	1.407	1.4085	1.4085	1.405
	1.470	1.472	1.45 + 1.487	1.463 + 1.478
$C_{8.4}MoF_6$	1.112	1.118		
τ_s = 0.106	1.30	1.301		
	1.398	1.394		
τ_I = 1.485	1.485	1.485		
	1.583	1.573		
	1.684	1.667		

for several models for the distorted lattices. In addition to the small shifts we also observe an intrinsic broadening of the diffraction lines, especially for the OsF_6-compound. This indicates that the domain-wall lattices have a finite correlation length, probably due to pinning effects. For C_9OsF_6 we find a correlation range of 60Å, whereas the range is close to the instrumental resolution of 250Å for the MoF_6-compound.

SUMMARY

It is tempting to associate the in-plane structure of the intercalant as measured by neutron scattering with the in-plane resistivity (note that the latter measure the domain size on the graphite layers). Our results strongly suggest smaller domain size for C_9OsF_6 from both resistivity and neutron scattering. However, the size of the domains are different in both measurements. We believe that the small intercalant domains in the case of C_9OsF_6 induce defects on the graphite layer. This effect and the charge localization found in this compound are probably responsible for the large residual resistivity of C_9OsF_6.

Summarizing, we find that the MF_6 GIC constitute a very interesting family of materials with intriguing chemical, electronic and structural properties and, clearly, considerably more study is needed before we can claim to understand these properties.

ACKNOWLEDGEMENTS

This work was supported by U.S.-Israel Binational Foundation grant 84-00192. Support from the Danish National Science Research Council is acknowledged. We wish to thank Dr. A.W. Moore of Union Carbide for the HOPG.

REFERENCES

1. D. Vaknin, D. Davidov, H. Selig, V. Zevin, I. Felner and Y. Yeshurun, Phys. Rev. B. 31 (1985) 3212.
   D. Vaknin, D. Davidov, V. Zevin and H. Selig, Phys. Rev. B. 35 (1987) 6423.
2. D. Vaknin, D. Davidov, H. Selig and Y. Yeshurun, J. Chem. Phys. 83 (1985) 3859.
3. I. Ohana, D. Vaknin, Y. Yacoby, H. Selig and D. Davidov, Phys. Rev. B. 35 (1987) 4522.
4. D. Vaknin, D. Davidov, H. Selig and D. Moses, Proceedings of 4th International Carbon Conference, Baden-Baden, F.R.G. (1986), pp. 514, 529.
5. S.E. Ulloa and G. Kirczenow, Phys. Rev. Lett. 56, (1986) 2537.
6. J.K. Kjems, Y. Yeshurun, D. Vaknin, D. Davidov and H. Selig, Phys. Rev. B 36, (1987) 6981.